A Solvation-Assisted Model for Estimating Anomeric Reactivity. Predicted versus Observed Trends in Hydrolysis of *n*-Pentenyl Glycosides[1]

C. Webster Andrews,[†,⊥] Robert Rodebaugh,[‡,§] and Bert Fraser-Reid*[,‡]

Division of Medicinal Chemistry, Glaxo Wellcome, Research Triangle Park, North Carolina 27709, and Paul M. Gross Chemical Laboratory, Duke University, Durham, North Carolina 27708

Received January 19, 1996[⊗]

An attempt has been made to predict qualitative trends in reactivity at the anomeric center, using *N*-bromosuccinimide-induced hydrolysis of *n*-pentenyl glycosides (NPGs) as the experimental model. Calculated relative activation energies based on internal energy differences between a reactant and the associated intermediate are not always in agreement with experimental observations. However, solvation energies obtained by the generalized Born surface area model in MacroModel developed by Still et al. give modified activation energies that are in excellent agreement with the experimentally observed trends. It is shown that the solvation model does not disturb the normally observed reactivity trends that can be rationalized on the basis of internal energies alone. The value of the methodology has been demonstrated for several substrates by first calculating their relative activation energies, then testing them experimentally, and finding excellent agreement with predictions.

Introduction

For laboratory syntheses of complex oligosaccharides in the current state of the art,[2] protecting groups must usually be stationed on the glycosyl donor and acceptor so as to enforce coupling at the desired site(s). Although some rules of engagement may be gleaned from literature precedents,[3] a prelude of trial and error is usually needed before the best partners can be ascertained. Such a procedure is wasteful of manpower, time, and resources, and the situation could be relieved if it were possible to evaluate, and thereby screen, potential partners computationally. Ideally such a computational tool would be useful (and used) only if it blended simplicity with reliability. The experimental tool should be similarly simple—ideally thin layer chromatography (TLC) or high-performance liquid chromatography (HPLC). This is the long-range objective of a program that has been initiated in our laboratory, and in this paper we describe some recent results.

Background

Although protecting groups prevent some sites from competing during a reaction, it is well-known that they can also profoundly affect the reactivity of the entire molecule.[4,5] Thus in 1988 we showed that such reactivity differences provide the basis of a protocol whereby two saccharides equipped with the same anomeric activating group could be coupled efficiently.[6] This plan, dubbed *armed/disarmed glycoside coupling*, has since been applied to a variety of glycosyl donors, showing that the phenomenon is not restricted[7] to the *n*-pentenyl glycosides[8] that had been used in our initial investigations. Furthermore, in 1991 we demonstrated that widely used cyclic acetals also affected anomeric reactivity to such an extent that an armed/disarmed strategy could be also be devised around them.[9] The latter phenomenon which arises from torsional strain complements the former which was ascribed to electronic factors.[10] Thus armed/disarmed strategies could be based upon either electronic or torsional considerations.

Other studies[11] designed to see if glycoside hydrolysis (a) involves boat conformations[12] and (b) requires that the leaving group be presented with an antiperiplanar lone pair[13] prompted us to carry out *ab initio* studies[11] to probe the energetics and preferred geometries for glycoside cleavage.[14] Axial and equatorial conformers of 2-methoxytetrahydropyran served as models for α- and

† Glaxo Wellcome.
‡ Duke University.
§ Winner of the Charles R. Hauser Fellowship, 1995−1996.
⊥ Present address: Natural Products and Glycotechnology (NPG) Research Institute, 4118 Swarthmore Rd, Durham, NC 27707.
⊗ Abstract published in *Advance ACS Abstracts,* July 1, 1996.
(1) We are grateful to the National Science Foundation (CHE 9311356) and Glaxo Research Institute for financial support of this work.
(2) For some recent reviews on oligosaccharide syntheses, see: Khan, S. H., O'Neil, R. A., Rahman, A., Eds. *Modern Methods in Carbohydrate Synthesis*; Harwood Academic Publishers: Amsterdam 1996. Fraser-Reid, B.; Madsen, R.; Campbell, A. S.; Roberts, C.; Merritt, J. R. In *Chemical Synthesis of Oligosaccharides*; Hecht, S. M., Ed.; Oxford University Press: Oxford, 1995, in press. Khan, S. H.; Hindsgaul, O. In *Frontiers in Molecular Biology*; Fukuda, M., Hindsgaul, O., Eds.; IRL Press: Oxford, 1994; p 206. Toshima, K.; Tatsuta, K. *Chem. Rev.* **1993**, 15031. Bonoub, J.; Boullanger, P.; Lafont, D. *Chem. Rev.* **1992**, *92*, 1167.
(3) For such a compilation that focuses on anomeric selectivity, see: Barresi, F.; Hindsgaul, O. *J. Carbohydr. Chem.* **1995**, *14*, 1043.
(4) See, for example: Paulsen, H. *Angew. Chem., Int. Ed. Engl.* **1982**, *21*, 155.
(5) See, for example: Mehta, S.; Andrewes, J. S. Johnston, B. D.; Svenson, B.; Pinto, B. M. *J. Am. Chem. Soc.* **1995**, *117*, 9783. Garegg, P. J.; Hutberg, H.; Wallin, S. *Carbohydr. Res.* **1982**, 10897.
(6) Mootoo, D. R.; Konradsson, P.; Udodong, U.; Fraser-Reid, B. *J. Am. Chem. Soc.* **1988**, *110*, 5583.
(7) See, for example: Roy, R.; Anderson, F. O.; Letellier, M. *Tetrahedron Lett.* **1992**, *33*, 6053. Sliedregt, L. A. J. M.; Zegelaar-Jaarsvald, K.; van der Marel, G. A.; van Boom, J. H. *Synlett* **1993**, 335. Boons, G. J.; Isles, S. *Tetrahedron Lett.* **1994**, *35*, 3593.
(8) Fraser-Reid, B.; Udodong, U. E.; Wu, Z.; Ottosson, H.; Merritt, R.; Rao, C. S.; Roberts, C.; Madsen, R. *Synlett* **1992**, 927.
(9) Fraser-Reid, B.; Wu, Z.; Andrews, C. W.; Skowronski, E.; Bowen, J. P. *J. Am. Chem. Soc.* **1991**, *113*, 1434.
(10) Fraser-Reid, B.; Wu, Z; Udodong, U. E.; Ottosson, H. *J. Org. Chem.* **1990**, *55*, 6068.
(11) Ratcliffe, A. J.; Mootoo, D. R.; Andrews, C. W.; Fraser-Reid, B. *J. Am. Chem. Soc.* **1989**, *111*, 7661.
(12) Deslongchamps, P. *Stereoelectronic Effects in Organic Chemistry;* Pergamon Press: New York, 1983; pp 30−35. Intramolecular Strategies and Stereochemical Effects: Glycosides and Orthoesters Hydrolysis Revisited. In *The Anomeric Effect and Associated Stereoelectronic Effects*; Thatcher, G. R. J., Ed.; ACS Symposium Series 539, American Chemical Society: Washington, D.C., 1993.
(13) Sinnott, M. L. *Adv. Phys. Org. Chem.* **1988**, *24*, 113.

S0022-3263(96)00122-3 CCC: $12.00

Scheme 1

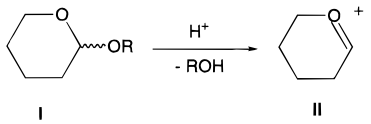

equation (i) Rel. E_a (g) = (Internal Energy)$_{II}$ - (Internal Energy)$_I$

equation (ii) Rel. ΔG_s = (Solvation Energy)$_{II}$ - (Solvation Energy)$_I$

equation (iii) Rel. E_a (s) = Rel. E_a (g) + Rel. ΔG_s

β-glycosides, respectively, and it was found that they were hydrolyzed through half-chair ($^4H_3$) and sofa (^4E) conformers and that they proceeded therefrom to oxocarbenium ions having the same conformations, respectively.[15]

Our calculations[15] also agreed with the well-known fact that β-glucosides generally react faster than their α-counterparts, the β/α ratio of ~2:1 being found to agree with experimentally obtained ratios for aqueous hydrolysis of some methyl glycosides.[16] However it should be noted that subsequent experiments by Wilson and Fraser-Reid have found that the β/α ratios can vary widely, depending on substitution and protecting group patterns.[17]

In connection with the above-described study concerning the effects of torsional strain on glycoside hydrolysis, we had attempted to correlate the experimentally observed times for hydrolysis with calculated activation energies computed with the PM3 semiempirical Hamiltonian.[19] The results were encouraging, but, not surprisingly, hardly adequate given the major approximations that had been made. For example, the activation energies were estimated to be the difference between internal energies of the glycoside **I** and the corresponding oxocarbenium ion **II** as shown in eq i, Scheme 1. This estimation involves the assumption that geometries of the *transition states* are the same as those of the associated glycosyl oxocarbenium ion intermediates, this approximation being justified on the grounds that transition states for glycoside hydrolyses are known to be late.[18] Additionally, our use of the PM3 Hamiltonian rendered this shortcut even more precarious owing to the fact that the resulting bond rotation barriers are very low,[19] as a result of which the structures obtained are rather flexible. Thus the oxocarbenium ions could distort away from the normal $^4H_3$ and ^4E ring conformations that are obtained at a higher level of theory.[15]

A second approximation, as is evident from Scheme 1 eq i, was to ignore solvation factors in order to simplify the calculations. This was not inconsequential, in view of the obvious expectation that the glycosides **I** and oxocarbenium ions **II** should have very different solvation energies and that protecting groups should have different solvation effects on **I** and **II**.

We now report that substantial improvements in the predictive value of the calculated energies are achieved by use of both internal and solvation energies of species **I** and **II**.

Scheme 2

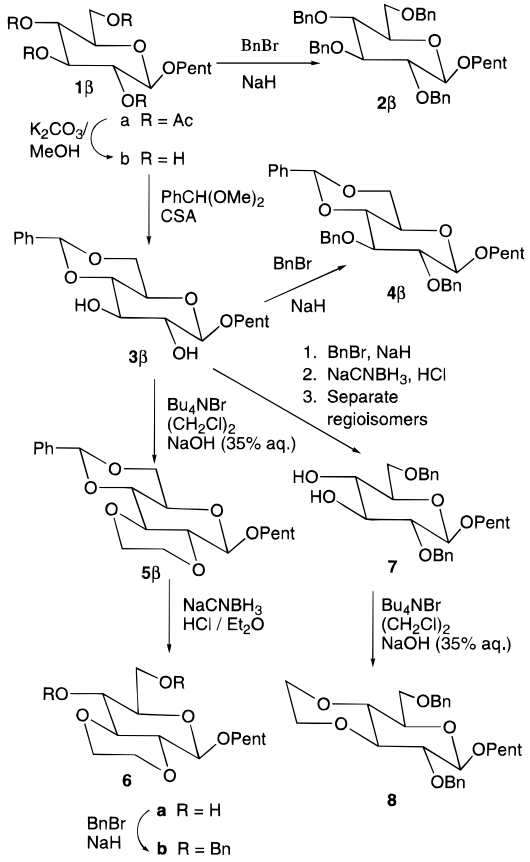

Synthesis of Substrates

It is well-known that α- and β-anomers (can) have different rates of hydrolysis, and in order to avoid this and other configurational effects, we initially confined our attention to derivatives of pent-4-enyl β-D-glucopyranoside (**1*β*b**). However, for reasons that will become clear below some α-D anomers (see Table 2) were subsequently studied. Compound **1*β*b** obtained by de-O-acetylation of pent-4-enyl 2,3,4,6-tetra-*O*-acetyl-β-D-glucopyranoside (**1*β*a**) was prepared by the procedure of Rodriguez and Stick.[20] Compounds **2**, **4**, **5**, **6b**, and **8** (Scheme 2) were prepared by routine procedures, or by adapting literature methods developed for the corresponding methyl glucosides.[21]

Ley's procedure[22] was followed for preparation of the dispiroketal (dispoke) derivatives **9** and **10** (Scheme 3), from which **11** and **12** were obtained without event. The structure of **11** was confirmed by X-ray analysis, and the ORTEP diagram is shown in Figure 1.

The benzylidene derivative **13** was problematic. We first attempted its preparation by treating the diol **3** with bisdihydropyran and camphorsulfonic acid in the usual way.[22] However these conditions caused cleavage of the benzylidene ring. Next an attempt was made to benzylidenate the dispoke diol **9** with α,α-dimethoxytoluene and camphorsulfonic acid, but cleavage of the dispoke moiety was now a major problem and only traces of **13** were obtained.

(14) Andrews, C. W.; Bowen, J. P.; Fraser-Reid, B. *J. Chem. Soc., Chem. Commun.* **1989**, 1913.
(15) Andrews, C. W.; Fraser-Reid, B.; Bowen, J. P. *J. Am. Chem. Soc.* **1991**, *113*, 8293.
(16) (a) See Table I in ref 15. (b) Isbell, H. S.; Frush, H. L. *J. Res. Natl. Bur. Std.* (*U.S.*) **1949**, *24*, 125.
(17) Wilson, B. G.; Fraser-Reid, B. *J. Org. Chem.* **1995**, *60*, 317.
(18) Bennett, A. J.; Sinnott, M. L. *J. Am. Chem. Soc.* **1986**, *108*, 7287.
(19) Stewart, J. J. *Comp.-Aided Mol. Design* **1990**, *4*, No. 1.
(20) Rodriquez, F. B.; Stick, R. V. *Austr J. Chem.* **1990**, *43*, 673.
(21) Cesare, P. D.; Gross, B. *Carbohydr. Res.* **1976**, 483. Garegg, P. J.; Iverson, T.; Oscarson, S. *Carbohydr. Res.* **1976**, *50*, C-12.
(22) Ley, S. V.; Leslie, R.; Tiffin, P. D.; Woods, M. *Tetrahedron Lett.* **1992**, *33*, 4767. Ley, S. V.; Boons, G.-J.; Leslie, R.; Woods, M.; Hollinshead, D. *Synthesis* **1993**, 689. Ley, S. V.; Downham, R.; Edwards, P. J.; Innes, J. E.; Woods, M. *Contemp. Org. Synth.* **1995**, *2*, 365.

Scheme 3

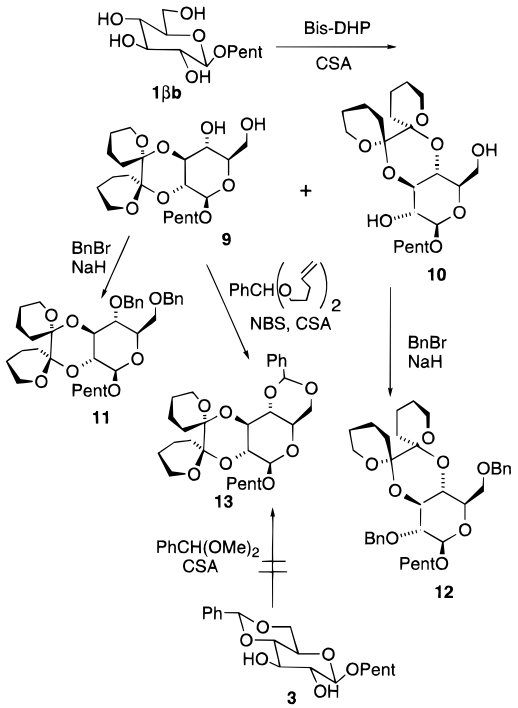

We next resorted to the bis(pent-4-enyl) acetal transfer reagents which have been recently developed in our laboratory for use under mild conditions.[23] In that report it was found that the acetalization reactions did proceed under the agency of *N*-halosuccinimides, but were greatly accelerated by trace amounts of protic or Lewis acids. Nevertheless the process has been shown to be driven by halonium ions—not by protons.[23] Accordingly, treatment of diol **9** with benzaldehyde bis(pent-4-enyl) acetal, NBS, and camphorsulfonic acid for 10 min at room temperature afforded a 72% yield of **13**.

For preparation of the α-anomers, D-glucose was subjected to Fischer glycosidation with pent-4-enol, and the product was acetylated in order to separate the anomers (Scheme 4). The desired α-anomers were then processed as described above for the corresponding *β*-counterparts.

Experimental Hydrolyses

The standard conditions for NBS-induced hydrolysis of the test substrates are described in detail in the Experimental Section. The times shown in Table 1, column 6, are for disappearance of the starting materials as judged by TLC, and these were subsequently confirmed by HPLC analysis of the crude reaction mixtures (see Experimental Section). These times are shown as relative data in column 7. (The data assembled in Tables 1 and 2 are simplified, more user-friendly versions of those presented in Table 3).

Calculated Activation Energies

It should be noted that the rigors of computing absolute activation energies are too involved to be undertaken in support of our synthetic work. The intent here is to obtain relative reactivities as an aid to synthesis. For the same reason, "reaction times" are determined by TLC and HPLC. The molecules under consideration are too large for geometry optimization with the 6-31G basis set or for post Hartree–Fock treatment necessary to deal with electron correlation.*[24,27]

In keeping with the work which had been done in our previous report,[15] the structures of the glycosides in Table 1 and their corresponding oxocarbenium ions were built using MacroModel[28] and subjected to PM3 geometry optimization and energy evaluation. The activation energies were calculated using eq i of Scheme 1 and then made relative to the reference compound **2*β***, the results being shown in column 2 of Table 1. It is seen that these energies correlate poorly with the experimentally observed hydrolysis times in column 7, since shorter reaction times should have correlated with lower activation energies.

Our method of estimating activation energies therefore needed to be improved. It was noted above that there are usually problems with PM3 calculations of oxocarbenium ion structures. By contrast, these structures are generally easily and reliably obtained by geometry optimizations using the 3-21G *ab initio* basis set and MacroModel starting structures.[28] A set of 3-21G activation energies was thereby obtained,[25,26] and once again, these were made relative to reference compound **2*β***, as shown in column 3 of Table 1. However, the results so obtained were found to follow the PM3 energies shown in column 2, which meant that the discrepancies with the experimental data had not been alleviated.

In a second attempt at improving the correlation, we decided to include solvation energies. As illustrated in Figure 2, solvation in water stabilized the oxocarbenium

(23) Madsen, R.; Fraser-Reid, B. *J. Org. Chem.* **1995**, *60*, 772.

(24) The relative activation energies in column 5 of Table 1, column 4 of Table 2, and the last column of Table 3 deserve comment. By calculating relative activation energies (equivalent to the use of isodesmic reactions involving reactants and intermediates), it is possible to cancel out many of the errors inherent in using low levels of theory.[25,26] The principal error is that electron correlation is ignored at the Hartree–Fock level for both ground states and oxocarbenium ions. However, the change in relative activation energy from molecule to molecule is quite large relative to the rate changes and reflects the fact that some errors are not cancelled out, as well as the fact that real electronic and steric differences exist. In the end, the *relative ordering*, which is what this study requires, is satisfactory. These relative activation energies (kinetic properties) should not be compared against known ground state energy differences (thermodynamic properties).

(25) Hehre, W. J.; Radom, P.; Schleyer, P. v. R.; Pople, J. A. *Ab Initio Molecular Orbital Theory*; John Wiley & Sons: New York, 1986 (see p 271, 298, 307).

(26) Wiberg, K. B.; Murcko, M. A. *J. Am. Chem. Soc.* **1989**, *111*, 4821. Jeffrey, G. A.; Pople, J. A.; Binkley, J. S.; Vishveshwara, S. *J. Am. Chem. Soc.* **1978**, *100*, 373. Andrews, C. W. Ph.D. Thesis, Duke University, 1989.

(27) Due to the cyclic nature of these compounds, conformational differences between solution and *in vacuo* are expected to be small. This allowed us to do *in vacuo* quantum mechanics with the expectation that the same conformation would be obtained in aqueous solution. This will not always be the case. A reviewer points out that a general scheme for more flexible molecules would be to do geometry optimization (or indeed, conformational searching) using one of the continuum solvation models that are now available in *semiempirical* or *ab initio* codes. A further assumption inherent in this work is that the single minimized conformation found for each structure (formally at 0 K) represents the ensemble of structures at the temperature of the rate determination. This is also reasonable due to the cyclic nature of the compounds. An additional point relates to the use of 6-31G* charges but not energies. High-level charges are required to obtain accurate solvation energies from the GB/SA model. Since the charges are not expected to change a great deal with geometry optimization, we used 6-31G*//3-21G charges and did not pursue 6-31G* geometry optimization (and more importantly, could not afford the cpu time involved). We did not use the single-point 6-31G* energies in the rate correlations because these energies are not minimized on the 6-31G* energy surface.

(28) Mohamadi, F.; Richards, N. G. J.; Guida, W. C.; Liskamp, R.; Caufield, C.; Chang, G.; Hendrickson, T.; Still, W. C. *J. Comput. Chem.* **1990**, *11*, 440.

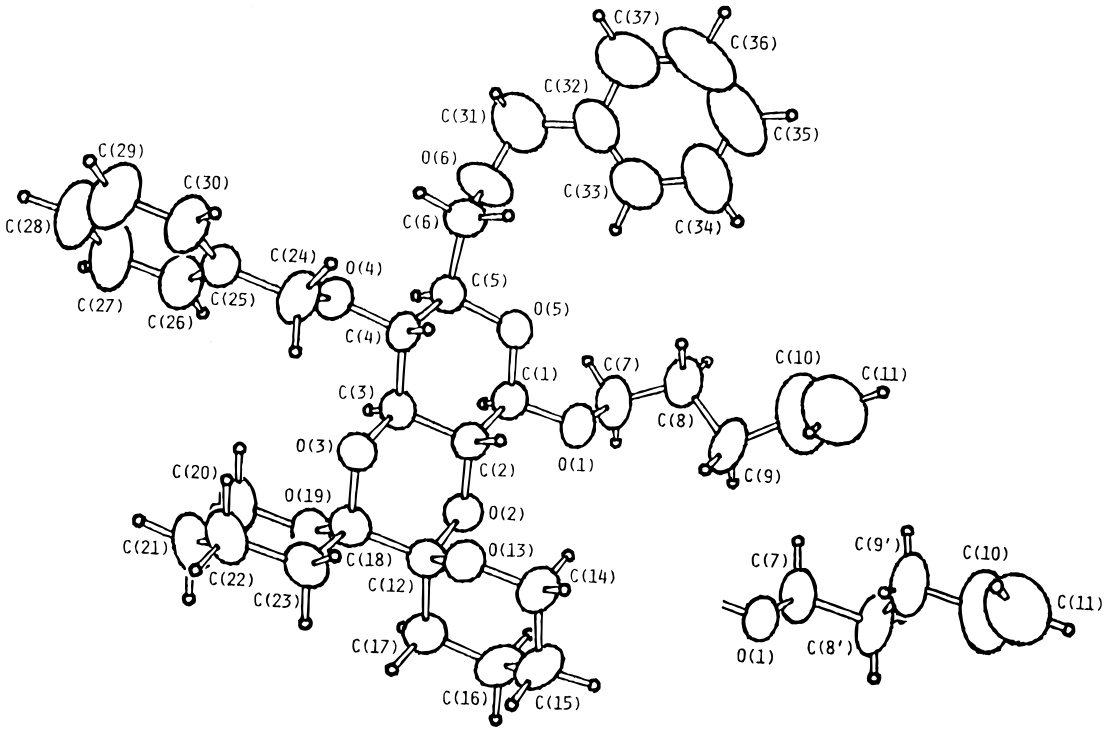

Figure 1. ORTEP diagram of the X-ray structure for pent-4-enyl 4,6-di-*O*-benzyl-2,3-*O*-(octahydro-2,2′-bi-2*H*-pyran-2,2′-diyl)-*β*-D-glucopyranoside (**11**). Diagram (40% probability ellipsoids) showing the crystallographic atom numbering scheme and solid-state conformation; C(8) and C(9) are disordered over two positions. Small circles represent hydrogen atoms.

Scheme 4

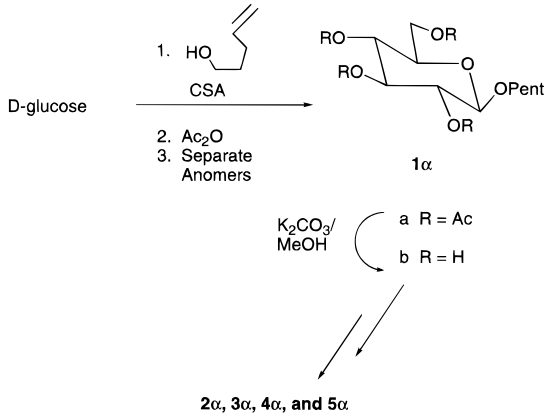

ion much more than the glycoside owing to the charged nature of the former. In the context of the thermodynamic cycle in Figure 3, we use the approximation that the internal energy change associated with activation, E_a (internal), is equal to the gas phase activation energy, E_a(g). Furthermore, the activation energy in solution E_a(s) is equal to E_a(internal) *modified* by solvation. It is clear that protecting groups influence the activation energy both from an internal energy standpoint, since some stabilize the oxocarbenium ion better than others, and from a solvation standpoint, since some are solvated better than others. The energy cycle in eq iv of Figure 3 has a net change of zero. The terms can be rearranged to yield an expression for the relative activation energy in solution composed of a term for the relative gas phase activation energy and another for the relative solvation energy shown in eq vi of Figure 3. The data resulting from eq vi are shown as rel E_a(s) in Tables 1 and 2.

Our solvation energies are calculated using the GB/SA solvation model of Still et al.[29] This is a two-term model. Term one consists of a cavity plus van der Waals energy and is a function of the conformation and solvent accessible surface area (SA) of the solute. Term two is an electrostatic polarization energy computed using generalized Born (GB) theory. Solvent is treated as a continuum, and explicit solvation is not required. A reasonable conformation and high-quality charges are necessary to compute an accurate GB/SA solvation energy.[29] High-quality charges require the use of a good basis set and electrostatic potential fitting, so we have used 6-31G* ESP-fit charges computed with the Pop = CHELPG option in the Gaussian 92 program.[30] The solute structures used are 3-21G-optimized, however, since the size of the dispoke protecting group prohibits 6-31G* geometry optimization.

The charges so obtained were used with the 3-21G-optimized structures to compute the solvation energy difference between reactant and reaction intermediate (see Scheme 1, eq ii) and then made relative to **2*β***. The relative solvation energy differences (rel ΔG_s) shown in column 4 of Table 1, were then added to the relative activation energies based on internal energies [rel E_a(g), i.e., column 3 of Table 1] to give the solvation-corrected activation energies [rel E_a(s), eq iii of Scheme 1 and column 5 of Table 1].

Arrhenius analyses,[31] done by plotting log of the reaction times in column 7 versus the activation energies before and after solvation correction, are shown in

(29) GB/SA solvation model: Still, W. C.; Tempczyk, A.; Hawley, R. C.; Hendrickson, T. *J. Am. Chem. Soc.* **1990**, *112*, 6127.

(30) Frisch, M. J.; Trucks, G. W.; Head-Gordon, M.; Gill, P. M. W.; Wong, M. W.; Foresman, J. B.; Johnson, B. G.; Schegel, H. B.; Robb, M. A.; Replogel, E. S.; Gomperts, R.; Andres, J. L.; Raghavachari, K.; Binkley, J. S.; Gonzalez, C.; Martin, R. L.; Fox, D. J.; Defrees, D. J.; Baker, J.; Stewart, J. J. P.; Pople, J. A. Gaussian Inc., Pittsburgh, PA, 1992.

(31) From the Arrhenius equation, plotting ln 1/*k* versus E_a gives a line with slope $1/RT = 1.7$ (at 300 K), and since reaction time is proportional to 1/*k*, ln(reaction time) is plotted against ΔE_a in Figure 4. Note, this is not a traditional Arrhenius analysis involving variation of temperature.

Table 1. NBS-Induced Hydrolysis of *n*-Pentenyl Glycosides: Computed and Observed Reactivity Trends Relative to 2β[a]

Column 1 Substrate	2 PM3	3 Rel. E_a (g)	4 Rel. ΔG_s	5 Rel. E_a (s)[b]	6 Time (h)[c]	7 Exp. t_{rel}[d]
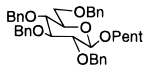 **2β**	0	0	0	0	2.3	1.0
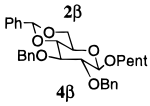 **4β**	---	6.1	-2.3	3.8	5.3	2.3
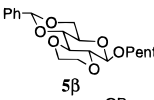 **5β**	11.9	11.5	-2.4	9.1	21.0	9.0
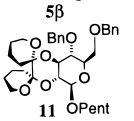 **11**	-6.8	-4.1	5.3	1.2	4.3	1.8
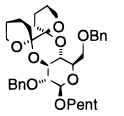 **12**	-2.4	-4.0	8.2	4.2	6.0	2.6
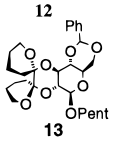 **13**	6.7	8.1	3.6	11.7	30.5	13.1

[a] For meaning of column headings, see Scheme 1. [b] Use of relative activation energy values means that structures with E_a' lower than that of **2β** will have negative rel E_a(s) values. [c] Experimental times given are ±0.2 h as verified by HPLC. Note: all relative energies in kcal. [d] In column 7, reaction times are shown relative to that for **2β**.

Figures 4a and 4b, respectively. It is clear that the latter is a vast improvement over the former, and that a distinctive trend has now emerged, the desired proportionality between predicted activation energies and observed reaction times being evident. The major difference between the solvated and unsolvated data in Figure 4 is that the activation energies for species **11**, **12**, and **13** (the dispoke derivatives) are not predicted well when solvation is ignored. Indeed, Figure 5 shows a linear regression line with an excellent R2 statistic (R2 = 0.98) indicating that the predicted activation energies explain well the experimental reaction times.[32]

Support of this conclusion is exemplified in the observations below.

Observations

(i) The torsional "disarm" effect of a 4,6-*O*-benzylidene group is apparent by comparing the E_a values for **2β** and **4β** in Table 1, which are 0 and 6.1 and 0 and 3.8 before and after solvation adjustment. The cyclic protecting group in **4β** raises the activation barrier by opposing the flattening that is required in the oxocarbenium ion.

(ii) The same trends, as in (i), are seen with **11** and **13**. Thus the rel E_a(s) sum values are 1.2 and 11.7, in agreement with the trend in the hydrolysis time ratio 1.8:13.1. The relative reaction time should decrease as the relative activation energy decreases.

(iii) The comparison between **5β** and **13** focuses on the effect of the dispoke protecting group. Thus, the internal activation energy in column 3 predicts that **13** should be hydrolyzed faster than **5β**, whereas the experimental observation in column 7 indicates the opposite. It is gratifying to see that the solvation adjusted values in column 5 predict that **13** should indeed react slower than **5β**. Thus, calculated and experimentally observed ratios in columns 5 and 7 show the same trends.

Table 2. Predicted Relative Reactivities of *n*-Pentenyl Glycosides: Importance of Solvation Contributions[a]

Column 1 Substrate	2 Rel. E_a (g)	3 Rel. ΔG_s	4 Rel. E_a (s)[b]	5 Time (h)[c]	6 Exp. t_{rel}
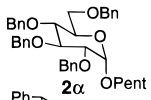 **2α**	0.8	0.3	1.1	3.9	1.7
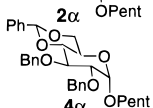 **4α**	8.7	-1.8	6.9	8.0	3.4
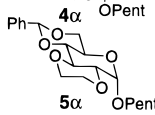 **5α**	15.6	-2.5	13.1	44.0	18.9
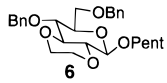 **6**	-0.7	0.1	-0.6	2.0	0.9
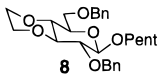 **8**	-2.5	0.3	-2.2	1.7	0.7

[a] For meaning of column headings, see Scheme 1. [b] Same as in Table 1. [c] Experimental times given are ±0.2 h as verified by HPLC. Note: all relative energies in kcal.

(iv) The 3-21G activation energies for the dispoke derivatives **11** and **12** (Table 1) were computed to be approximately the same, −4.1 and −4.0, respectively, which implied that both should be hydrolyzed *faster* than the reference material **2β**. On the other hand, the corresponding experimentally observed values in column 7 showed (a) that **11** was hydrolyzed faster than **12** and (b) that both were *slower* than **2β**. However, as shown in column 5, by allowing for solvation energies, both observations, namely, the slower reaction of **11** and **12** *vis-a-vis* **2β** and the greater reactivity of **11** *vis-a-vis* **12**, are qualitatively predicted.

Items i−iv above relate to the results in Table 1, where the calculated energies were determined *after* the experimental data had been obtained. It was therefore important to see whether the calculations would have a predictive value. Accordingly, the molecules in Table 2 were designed to test two predictions: (a) first, that α-anomers react more slowly than β-anomers; (b) second, that by breakdown of the data in Table 1, the disarming effect of a dispoke protecting group can be dissected into electronic and solvation factors. Thus for **11** and **12**, column 3 shows arming electronic effects (−4.1 and −4.0 kcal, respectively) while column 4 shows disarming solvation effects (i.e., positive contributions, 5.3 and 8.2 kcal, respectively). The same trends are observed for **5β** and **13**, in that the dispoke residue in the latter lowers the electronic energy difference from 11.5 to 8.1 kcal but raises the solvation energy difference from −2.4 to 3.6 kcal.

(v) It is significant to note that the activation energy values [rel E_a(g) and rel E_a(s)] in Tables 1 and 2 predict correctly that **2β**, **4β**, and **5β** are hydrolyzed faster than **2α**, **4α**, and **5α**, respectively—in keeping with well-known experimental evidence[11] and our previous calculations.[15] Thus, the predicted activation energies for the α-anomers are greater than those for the β-anomers.

(vi) Comparison of **11** and **12** in Table 1 with **6** and **8**, respectively, in Table 2 bears out prediction (b) above that the dispoke protecting group is disarming. Thus, removal of dispoke from **11** gives **6**, which is more disarmed (i.e., internal energy barrier is *raised* from −4.1 to −0.7 kcal)

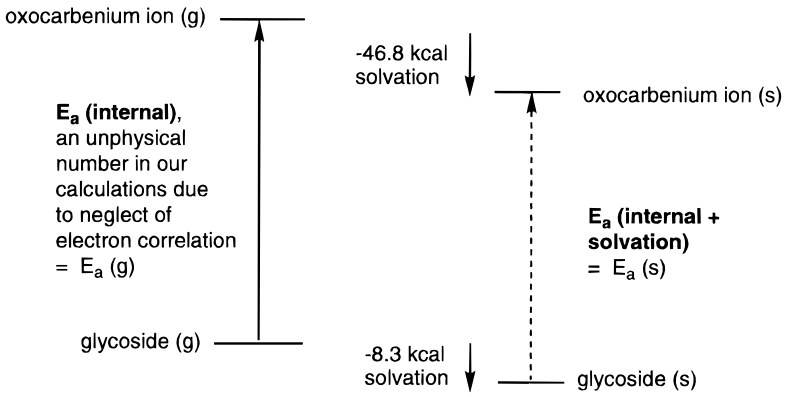

Figure 2. Impact of solvation on the activation energy of glycoside hydrolysis for substrate **2*β***. Solvation in water stabilizes the oxocarbenium ion much more than the glycoside due to the fact that the oxocarbenium ion is charged (via protonation). In the context of the thermodynamic cycle below, we use the approximation that the internal energy change associated with activation, E_a(internal), is equal to the gas phase activation energy, E(g). Furthermore, the activation energy in solution E(s) is equal to E(internal) modified by solvation. Protecting groups influence the activation energy both from an internal energy standpoint, since some stabilize the oxocarbenium ion better than others, and from a solvation standpoint, since some are solvated better than others.

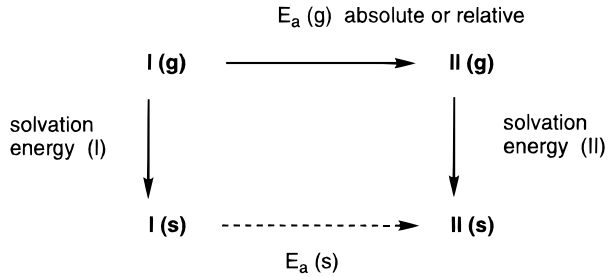

equation (iv) $0 = E_a(g) + \text{solvation energy II} - E_a(s) - \text{solvation energy I}$

equation (v) $E_a(s) = E_a(g) + (\text{solvation energy II} - \text{solvation energy I})$

equation (vi) $\underbrace{\text{relative } E_a(s)}_{\text{column 5}} = \underbrace{\text{relative } E_a(g)}_{\text{column 3}} + \underbrace{(\text{solvation energy II} - \text{solvation energy I})}_{\text{column 4}}$

Figure 3. Thermodynamic cycle applied to activation energies. The energy cycle has a net change of zero. The terms can be rearranged to correspond to the columns in Table 2. Species I is the glycoside and species II is the oxocarbenium ion, based on the approximation that the energy of the oxocarbenium ion is similar to the energy of the transition state. In the general case, species I is the reactant and species II is the transition state. The activation energies can be absolute (v) or relative (vi). Column numbers refer to Table 1.

but has a *lower* solvation energy difference (5.3 → 0.1 kcal). Similarly, in going from **12** to **8**, the structure becomes more disarmed electronically (−4.0 → −2.5 kcal) but is better solvated (8.2 → 0.3 kcal). In both cases, the dispoke group is disarming because of its poor solvation.

(vii) It is possible to further pinpoint the origin of some of these effects by breakdown of the solvation energy data in Table 3. Thus, these solvation energy values indicate that in the case of **11**, **12**, and **13** ionic intermediate **II** is *relatively* less stabilized *vis-a-vis* the corresponding starting glycoside **I**, than is the case with the non-dispoke substrates. *The result in item vii confirms the finding in item vi, that it is difficult to solvate a glycosyl cation containing a dispoke protecting group.*

Evidence in support of the foregoing conclusion is found in the data for **5*β*** and **13**, Table 1. These compounds differ only in the fact that the O2−O3 bridge is more difficult to solvate in **13** than in **5*β***. The energy values in column 3 indicate that **13** should be hydrolyzed faster than **5*β***—which is opposite to the experimentally obtained results in column 7. Inspection of the values in column 4 reveal that the effect of solvation is to increase the activation energy of **13** but to decrease that of **5*β***. Inclusion of these adjustments (see column 5) now correctly predicts the observed faster hydrolysis of **5*β***.

From the result in item v, it is gratifying to see that the solvation model does not disturb the normal trends in reactivity ($\beta > \alpha$) that are based on internal energies.

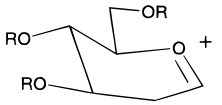

^{4}E sofa

III

Finally, the disarming effect of a 4,6-*O*-benzylidene

(32) The treatment shown in footnote 31 predicts a slope of 1.7. However, the slope in Figure 5 is 0.21, owing to the fact that the regression analysis compensates for the exaggerated 3-21G activation energies.[24] Hehre et al. have shown the need for electron correlation in reactivity modeling[25] which has not been addressed in this study.

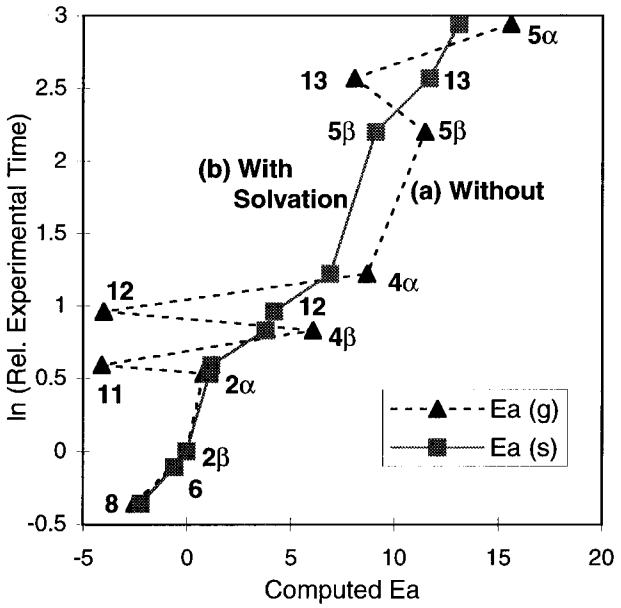

Figure 4. Plot of ln(rel experimental time) vs computed E_a (a) without solvation and (b) with solvation. (a) = Table 1 (ln-[column 7] vs 3) or Table 2 (ln[column 6] vs 2). (b) = Table 1 (ln[column 7] vs 5) or Table 2 (ln[column 6] vs 4).

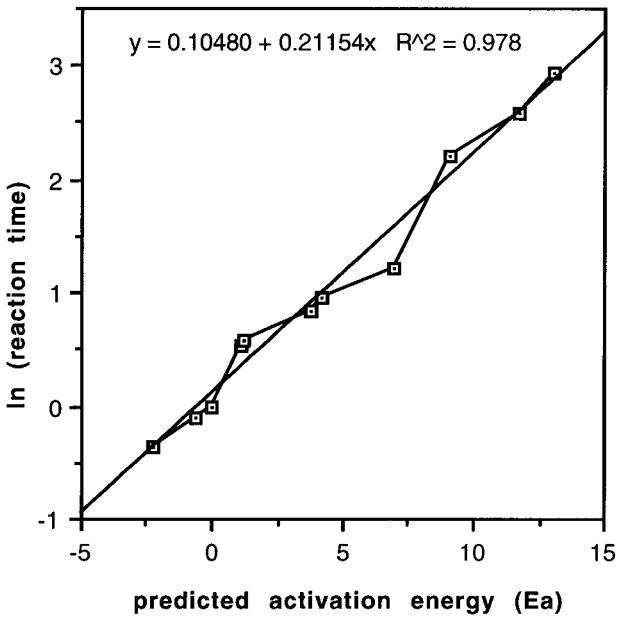

Figure 5. Arrhenius analysis of glycoside hydrolysis data.

ring was discussed in items i and ii above. By contrast, could bridging cyclic protecting group have an *arming* effect if poor solvation could be avoided? Our 6-31G* calculations[15] had shown that β-glycosides hydrolyze through a ^4E sofa transition state, **III.** If so, a *trans*-fused 6-membered ring should impede reactivity at C2/C3 much more than at C3/C4—a fact which is obvious from simple chemical models. Indeed the data for regioisomers **6** and **8** (Table 2) indicate that in both cases the rings reduce the internal activation energies (rel E_a = −0.7 and −2.5, respectively) relative to **2*β***. *However, the C3/C4 ring is so effective that it may be considered to have an arming effect.* Unfortunately, the experimental values in column 6 for **6** and **8** do not reflect this dramatic difference, suggesting that there is more work to be done. Further testing of the solvation model is therefore underway and will be reported in due course.

Experimental Section

General. Please see ref 17 for general procedures.

General Procedure for Hydrolysis Studies. Rate studies on the *n*-pentenyl glycosides were carried out by accurately weighing 25−50 mg of the glycosides into separate flasks wrapped in aluminum foil. An accurately weighed amount of NBS was added to a standard solution of 1% H_2O/MeCN to make a solution that contained 3 mmol of NBS in 40 mL of solution. Portions of this solution (40 mL per mmol glycoside) were pipetted into the reaction flasks and the mixtures stirred at room temperature. The reaction times were measured by TLC (4:1 light petroleum ether: EtOAc) by looking for the disappearance of the starting materials. Relative times were then calculated on the basis of absolute reaction times.

In order to confirm that all of the starting material had reacted fully, an aliquot of each reaction was quenched by

Table 3. Internal and Solvation Energies[a] Calculated by PM3 and 3-21G Programs

	internal energies						solvation energies GB/SA (kcal)			internal plus solvation energies (kcal)
	PM3 (kcal)			3-21G (kcal)						
structure	energy	E_a(g) internal	rel E_a(g) internal	energy	E_a(g) internal	rel E_a(g) internal	solvation energy	ΔG_s	rel ΔG_s	rel E_a(a)
2*β*	−237.6	235.2	0	−873.604 54	114.100 27	0	−8.3	−38.5	0	0
	−2.4			−759.504 27			−46.8			
4*β*				−833.640 04	114.109 92	6.1	−9.7	−40.8	−2.3	3.8
				−719.530 12			−50.5			
4*β*	−224	247.1	11.9	−832.480 95	114.116 83	11.5	−12.6	−40.9	−2.4	9.1
	23.1			−718.362 32			−53.5			
11	−322.6	228.4	−6.8	−1329.611 18	114.093 76	−4.1	−9.7	−33.2	5.3	1.2
	−94.2			−1215.517 42			−42.9			
12	−323.6	232.8	−2.4	−1329.613 35	114.093 93	−4	−13.4	−30.3	8.2	4.2
	−90.6			−1215.519 42			−43.7			
13	−316.6	241.9	6.7	−1289.648 39	114.113 16	8.1	−10	−34.9	3.6	11.7
	−74.7			−1175.535 23			−44.9			
6				−872.448 09	114.099 18	−0.7	−11	−38.4	0.1	−0.6
				−758.347 37			−49.4			
8				−872.448 09	114.096 31	−2.5	−10.5	−38.2	0.3	−2.2
				−758.351 79			−48.7			
4α				−873.605 75	114.101 48	0.8	−8.6	−38.2	0.3	1.1
				−759.504 27			−46.8			
4α				−833.644 33	114.114 21	8.7	−10.2	−40.3	−1.8	6.9
				−719.530 12			−50.5			
5α				−832.487 48	114.125 16	15.6	−12.5	−41	−2.5	13.1
				−718.362 32			−53.5			

[a] The energy values are shown in pairs: the upper one for the glycoside and the lower one for the corresponding oxocarbenium ion.

treatment with 10% aqueous $Na_2S_2O_3$. Extraction of this aqueous layer with CH_2Cl_2 was then performed, followed by extraction of the organic phase with brine. The CH_2Cl_2 extract was dried (Na_2SO_4), filtered, and evaporated in *vacuo*. The residue was then analyzed for the presence of starting materials *via* injection onto a Rainin Dynamax HPLC column.[17]

Pent-4-enyl 2,3,4,6-Tetra-*O*-acetyl-α-D-glucopyranoside (1αa). Camphorsulfonic acid (300 mg) was added to a mixture of D-glucose (25.0 g, 139 mmol) and 4-penten-1-ol (80 mL). The mixture was heated at 100 °C for 3 days under argon. The reaction was quenched with Et_3N, and the bulk of the pentenyl alcohol was distilled under vacuum using a dry ice condenser. The residue was purified by flash chromatography (5 → >10% methanol/CH_2Cl_2) to yield the pentenyl glucoside as a dark orange oil (18.58 g, 75 mmol, 54%). This material was dissolved in pyridine (80 mL) under argon, acetic anhydride (42 mL, 450 mmol) was added, and the solution was stirred overnight. The reaction was quenched by addition of methanol, and the solvent was evaporated under high vacuum. The residue was azeotroped with toluene (3 × 200 mL) and then flash chromatographed (20 → 30% EtOAc/petroleum ether) to give **1αa** (16.83 g, 40.4 mmol, 54%) and **1βa** (4.02 g, 9.65 mmol, 13%) and a mixture (ca. 2:1 β: α) of anomers (8.65 g, 20.8 mmol, 28%). For **1αa**: mp 62−63 °C (petroleum ether/ethyl ether); $[\alpha]^{21}_D$ +124° (*c* 1.12, $CHCl_3$); ^{1}H NMR δ 1.65 (m, 2H), 2.00−2.12 (4 s, 12H), 2.14 (m, 2H), 3.41 (ddd, 1H), 3.68 (ddd, 1H), 4.00 (m, 1H), 4.08 (dd, 1H), 4.23 (dd, 1H), 4.83 (dd, J = 3.74 Hz, 1H), 4.94−5.15 (m, 4H), 5.46 (t, 1H), 5.79 (m, 1H); ^{13}C NMR δ 170.57, 170.09, 169.55, 137.65, 115.30, 95.63, 70.84, 70.15, 68.54, 67.78, 67.10, 61.86, 30.03, 28.34, 20.98, 20.65.

Anal. Calcd for $C_{19}H_{28}O_{10}$: C, 54.80; H, 6.78. Found: C, 54.85; H, 6.83.

4-Pentenyl 2,3,4,6-Tetra-*O*-acetyl-β-D-glucopyranoside (1βa). Following the procedure of Rodriquez and Stick,[20] tetra-*O*-acetyl-α-D-glucopyranosyl bromide (24.87 g, 60.48 mmol) and 4-penten-1-ol (18.3 mL, 2.5 equiv) were dissolved in dry, distilled CH_2Cl_2 (130 mL) under argon. Powdered, freshly activated 4 Å molecular sieves (30 g) were added, and the mixture was stirred for 30 min. Silver carbonate (20.34 g, 73.76 mmol, 1.2 equiv) was quickly added, and the reaction was stirred under darkness for 72 h. The reaction mixture was then diluted with CH_2Cl_2 (150 mL), filtered through a wet Celite pad, and washed consecutively with saturated aqueous $NaHCO_3$ (2 × 125 mL) and brine (1 × 150 mL). The organic layer was dried over anhydrous Na_2SO_4, concentrated, and flash chromatographed (85:15 → 60:40 petroleum ether/EtOAc) to give **1βa** (20.05 g, 76%) as a white solid: R_f 0.48 (3:2 petroleum ether/EtOAc); $[\alpha]_D$ −19.5° (*c* 1.06, $CHCl_3$) [lit.[20] = −19.4°], mp 47−48 °C (petroleum ether:diethyl ether) [lit.[20] mp 45−46 °C]; ^{1}H NMR ($CDCl_3$) δ 1.69−1.61 (m, 2H), 1.99 (s, 3H), 2.02 (s, 3H), 2.05 (s, 3H), 2.09 (s, 3H), 3.46 (m, 1H), 3.67 (m, 1H), 3.85 (m, 1H), 4.13 (dd, J = 2.44 Hz, 1H), 4.24 (dd, J = 4.68 Hz, J = 12.24 Hz, 1H), 4.48 (d, J = 7.92 Hz, 1H), 4.94 (m, 2H), 5.01 (m, 1H), 5.05 (t, 1H), 5.18 (t, J = 9.55 Hz, 1H), 5.78 (m, 1H); ^{13}C NMR ($CDCl_3$) δ 170.70, 170.32, 169.41, 169.29, 137.79, 115.10, 100.81, 72.85, 71.66, 71.35, 69.33, 68.39, 61.96, 29.81, 28.54, 20.77, 20.69, 20.64, 20.58.

Anal. Calcd for $C_{19}H_{28}O_{10}$: C, 54.80, H, 6.78; Found: C, 54.80, H, 6.80.

Pent-4-enyl 2,3,4,6-Tetra-*O*-benzyl-α-D-glucopyranoside (2α). To a solution of pent-4-enyl 2,3,4,6-tetra-*O*-acetyl-α-D-glucopyranoside (**1αa**) (16.83 g, 40.4 mmol) in anhydrous methanol (90 mL) was added K_2CO_3 (2.02 g), and the mixture was stirred overnight at room temperature. The solution was neutralized with Amberlite IR-120 (H^+), filtered through Celite and concentrated. The residue, **1αb**, was flash chromatographed (7 → 13% MeOH/CH_2Cl_2) to give the tetrol as a clear colorless oil (9.66 g, 97%). A portion of this material (1.01 g, 4.07 mmol) was then dissolved in DMF (20 mL) under argon cooled to 0 °C, and the solution was treated with sodium hydride (586 mg, 24.4 mmol) and benzyl bromide (2.9 mL, 24 mmol) and allowed to warm to room temperature while stirring overnight. The reaction was quenched with methanol, diluted with ether (75 mL), and washed with water (1 × 40 mL). The organic phase was washed with saturated aqueous $NaHCO_3$ (1 × 50 mL) and brine (1 × 45 mL), dried (Na_2SO_4), filtered, and concentrated. The crude residue was purified by flash chromatography (10 → 15% EtOAc/petroleum ether) to give **2α** as a colorless oil (2.106 g, 3.46 mmol, 85%): $[\alpha]^{21}_D$ +33.1° (*c* 1.34, $CHCl_3$); ^{1}H NMR δ 1.77 (m, 2H), 2.18 (m, 2H), 3.44 (dd, 1H), 3.58−3.85 (m, 6H), 4.02 (m, 1H), 4.53 (m, 2H), 4.67 (m, 2H), 4.70−4.78 (m, 4H), 4.98−5.07 (m, 3H), 5.85 (m, 1H), 7.13−7.48 (m, 20H); ^{13}C NMR δ 138.93, 138.35, 138.26, 138.11, 137.98, 128.49, 128.24, 128.20, 127.99, 127.75, 127.65, 114.94, 97.02, 82.14, 80.15, 77.78, 75.77, 75.14, 73.51, 73.25, 70.15, 68.50, 67.53, 30.33, 28.59.

Anal. Calcd for $C_{39}H_{44}O_6$: C, 76.95; H, 7.28. Found: C, 76.81; H, 7.25.

4-Pentenyl 2,3,4,6-Tetra-*O*-benzyl-β-D-glucopyranoside (2β). To a solution of 4-pentenyl 2,3,4,6-tetra-*O*-acetyl-β-D-glucopyranoside (**1βa**) (6.58 g, 15.8 mmol) in anhydrous methanol (50 mL) was added a catalytic amount of K_2CO_3 (ca. 200 mg), and the mixture was stirred for 4.5 h. The reaction mixture was filtered through a Celite pad and concentrated to give crude pentenyl glucoside **1βa** as a yellow foam. To a stirred solution of this material in DMF at 0 °C under argon was added NaH (60% dispersion, 3.16 g, 79 mmol, 5 equiv). Benzyl bromide (11.3 mL, 6 equiv) was added dropwise at 0 °C, and the mixture was then stirred at room temperature overnight. The reaction was quenched with methanol, diluted with diethyl ether (200 mL), and washed consecutively with cold H_2O (1 × 150 mL), saturated aqueous $NaHCO_3$ (2 × 100 mL), and brine (2 × 100 mL). The organic layer was dried over $MgSO_4$, filtered, concentrated *in vacuo*, and the residue was flash chromatographed (95:5 → 90:10 petroleum ether/EtOAc) to yield **2β** as a white solid (10.0630 g, 10.74 mmol, 68% yield from **1βa**). R_f 0.69 (4:1 petroleum ether/EtOAc); $[\alpha]_D$ +5.48° (*c* 1.06, $CHCl_3$); mp 70−71 °C (ethanol); ^{1}H NMR ($CDCl_3$) δ 1.72 (m, 2H) 2.11 (m, 2H), 3.38 (m, 1H), 3.45−3.69 (m, 5H), 3.91 (m, 1H), 4.32 (d, J = 7.76 Hz, 1H), 4.50−4.61 (m, 4H), 4.78 (m, 3H), 4.98 (m, 4H), 5.82 (m, 1H), 7.35 (m, 20H); ^{13}C NMR ($CDCl_3$) δ 138.67, 138.48, 138.21, 138.10, 128.42, 128.29, 128.03, 127.92, 127.81, 127.64, 114.97, 103.67, 89.8, 84.76, 82.30, 77.94, 75.77, 75.08, 74.91, 73.53, 69.42, 30.32, 29.04.

Anal. Calcd for $C_{39}H_{44}O_6$: C, 76.95, H, 7.28. Found: C, 76.74, H, 7.33.

Pent-4-enyl 4,6-*O*-Benzylidene-α-D-glucopyranoside (3α). To a solution of pentenyl α-glucoside **1αb** (1.2875 g, 5.2 mmol) in DMF (12 mL) were added PPTS (50 mg) and benzaldehyde dimethyl acetal (0.898 mL, 5.98 mmol). The mixture was heated at 80 °C for 3.5 h under a stream of argon to remove methanol. The reaction was quenched with Et_3N (10 drops), concentrated under high vacuum, and flash chromatographed (25 → 30% EtOAc/CH_2Cl_2) to give **3α** as a white crystalline solid (1.6417 g, 4.87 mmol, 94%): mp 90 °C (ethyl acetate/petroleum ether); $[\alpha]^{21}_D$ +96.5° (*c* 1.13, $CHCl_3$); ^{1}H NMR δ 1.73 (m, 2H), 2.14 (m, 2H), 2.27−2.88 (broad s, 2H), 3.48 (m, 2H), 3.57 (dd, 1H), 3.65−3.88 (m, 4H), 3.89 (t, 1H), 4.25 (dd, 1H), 4.85 (d, J = 3.93 Hz, 1H), 4.97−5.09 (m, 2H), 5.51 (s, 1H), 5.79 (m, 1H), 7.31−7.50 (m, 5H); ^{13}C NMR δ 137.82, 137.04, 129.26, 128.34, 126.33, 115.27, 101.90, 98.76, 80.92, 72.91, 71.83, 68.93, 67.96, 62.62, 30.35, 28.58.

Anal. Calcd for $C_{18}H_{24}O_6$: C, 64.27; H, 7.19. Found: C, 64.10; H, 7.21.

Pent-4-enyl 4,6-*O*-Benzylidene-β-D-glucopyranoside (3β). Pent-4-enyl β-D-glucopyranoside (**1βb**) (7.2000 g, 28.92 mmol) was treated as described above for **3α**. The crude residue was flash chromatographed (3:2 EtOAc/petroleum ether) to give **3β** (4.766 g, 49%) as a white solid: $[\alpha]^{21}_D$ −43.8° (*c* 1.16, $CHCl_3$); mp 144−145 °C (ethanol); ^{1}H NMR ($CDCl_3$) δ 1.71 (m, 2H), 2.11 (m, 2H), 3.02 (s, 1H), 3.20 (s, 1H), 3.38−3.59 (m, 4H), 3.74 (m, 2H), 3.88 (ddd, 1H), 4.25−4.36 (m, J = 7.62 Hz, J = 4.82 Hz, 2H), 4.92−5.11 (m, 2H), 5.49 (s, 1H), 5.81 (m, 1H), 7.31−7.50 (m, 5H); ^{13}C NMR δ 137.98, 137.00, 129.29, 128.36, 126.32, 115.09, 103.19, 101.90, 80.57, 74.53, 73.10, 69.88, 68.68, 66.35, 30.12, 28.71.

Anal. Calcd for $C_{18}H_{24}O_6$: C, 64.27,; H, 7.19. Found: C, 64.10; H, 7.23.

Pent-4-enyl 2,3-Di-*O*-benzyl-4,6-*O*-benzylidene-α-D-glucopyranoside (4α). To a solution of pent-4-enyl 4,6-*O*-benzylidene-α-D-glucopyranoside (**3α**) (1.16 g, 3.43 mmol) in

DMF (14 mL) under argon at 0 °C was added sodium hydride (394.5 mg of a 60% dispersion in mineral oil, 10.3 mmol), and after 15 additional minutes benzyl bromide (1.22 mL, 10.3 mmol) was added. The solution was allowed to warm to room temperature and gradually stirred overnight. The reaction was then quenched with glacial acetic acid and taken up in diethyl ether (125 mL). The ether layer was successively washed with H_2O (2 × 75 mL), saturated aqueous $NaHCO_3$ (2 × 75 mL), and brine (1 × 75 mL). The organic phase was dried (Na_2SO_4), filtered, and concentrated. The residue was flash chromatographed (7 → 15% EtOAc/petroleum ether) to give **4α** as a white crystalline solid (1.6058 g, 3.09 mmol, 90%): mp 82−83 °C (ethanol); $[\alpha]^{21}_D$ +0.74° (*c* 5.52, $CHCl_3$); ^{1}H NMR δ 1.76 (m, 2H), 2.17 (m, 2H), 3.46 (ddd, 1H), 3.51−3.76 (m, 4H), 3.88 (ddd, H-5), 4.05 (t, 1H), 4.27 (dd, 1H), 4.72 (m, 2H, *J* = 3.77 Hz, 1H), 4.79−5.10 (m, 5H), 5.58 (s, 1H), 5.81 (m, 1H), 7.21−7.53 (m, 15H); ^{13}C NMR δ 138.81, 138.27, 137.92, 137.36, 128.88, 128.39, 128.26, 128.19, 127.93, 127.80, 127.51, 125.97, 115.00, 101. 18, 98.02, 82.21, 79.38, 78.59, 75.28, 73.50, 69.04, 67.66, 62.38, 30.21, 28.49.

Anal. Calcd for $C_{32}H_{36}O_6$: C, 74.39; H, 7.02. Found: C, 74.21; H, 7.03.

Pent-4-enyl 2,3-Di-*O*-benzyl-4,6-*O*-benzylidene-*β*-D-glucopyranoside (4*β*). Pent-4-enyl 4,6-*O*-benzylidene-*β*-D-glucopyranoside (**3*β***) (2.20 g, 6.54 mmol) was benzylated as described above for **4α**. The residue was flash chromatographed (95:5 petroleum ether/EtOAc) to yield **4*β*** as a clear oil which crystallized overnight under vacuum (2.7368 g, 5.30 mmol, 81%): $[\alpha]^{21}_D$ −36.4° (*c* 1.05, $CHCl_3$); mp 76 °C (ethanol); ^{1}H NMR δ 1.75 (m, 2H), 2.16 (m, 2H), 3.37−3.48 (m, 2H), 3.58 (ddd, 1H), 3.64−3.81 (m, 3H), 3.95 (ddd, 1H), 4.34 (dd, *J* = 4.91 Hz, *J* = 10.45 Hz, 1H), 4.49 (d, *J* = 7.76 Hz, 1H), 4.78 (m, 2H), 4.88−5.04 (m, 4H), 5.56 (s, 1H), 5.80 (m, 1H), 7.21−7.53 (m, 15H); ^{13}C NMR δ 138.54, 138.36, 137.94, 137.36, 128.98, 128.37, 128.33, 128.15, 128.10, 127.77, 127.68, 126.05, 115.11, 104.15, 101.13, 82.17, 81.54, 80.93, 75.44, 75.19, 69.86, 68.85, 66.04, 30.22, 28.99.

Anal. Calcd for $C_{32}H_{36}O_6$: C, 74.39; H, 7.02. Found: C, 74.35; H, 7.02.

Pent-4-enyl 4,6-*O*-Benzylidene-2,3-*O*-ethylene-α-D-glucopyranoside (5α). To pent-4-enyl 4,6-*O*-benzylidene-α-D-glucopyranoside (**3α**) (469 mg, 1.39 mmol) were added tetrabutylammonium bromide (89.6 mg, 0.278 mmol) and dichloroethane (6 mL) according to the published method.[21] An aqueous solution of NaOH (35%, 7 mL) was added, and the mixture was stirred rapidly at 50 °C for 24 h. At this time, fresh NaOH (35% aq, 4 mL) was added, and the mixture was stirred for an additional 24 h. The mixture was cooled and partitioned between H_2O:Et_2O (1:1; 125 mL), and the H_2O layer was re-extracted with Et_2O (2 × 50 mL) and EtOAc (1 × 50 mL). The organic layers were combined, extracted with brine (1 × 100 mL), dried (Mg_2SO_4), and concentrated to a yellow oil. The oil was flash chromatographed (3:1 petroleum ether/EtOAc) to yield **5α** (463.1 mg, 1.27 mmol, 92%) as a clear, slightly yellow oil: $[\alpha]^{21}_D$ +63.2° (*c* 1.37, $CHCl_3$); ^{1}H NMR δ 1.76 (m, 2H), 2.16 (m, 2H), 3.50 (m, 3H), 3.60−4.01 (m, 10H), 4.32 (dd, 1H), 4.88 d, *J* = 3.42 Hz, 1H), 4.98 (m, 2H), 5.52 (s, 1H), 5.81 (m, 1H), 7.32−7.50 (m, 5H); ^{13}C NMR δ 137.89, 136.97, 129.21, 128.31, 126.46, 115.17, 102.10, 97.49, 79.33,-77.37, 73.90, 69.03, 67.78, 67.53, 66.45,63.22, 30.22, 28.53.

Anal. Calcd for $C_{20}H_{26}O_6$: C, 66.28; H, 7.23. Found: C, 66.19; H, 7.25.

Pent-4-enyl 4,6-*O*-Benzylidene-2,3-*O*-ethylene-*β*-D-glucopyranoside (5*β*). Pent-4-enyl 4,6-*O*-benzylidene-*β*-D-glucopyranoside (**3*β***) (418.9 mg, 1.24 mmol) was subjected to the phase transfer reactions described for **5α**. The crude product was flash chromatographed (3:1 petroleum ether/EtOAc) to yield **5*β*** (275 mg, 0.756 mmol, 61%) as a white solid: $[\alpha]^{21}_D$ −62.8° (*c* 1.01, $CHCl_3$); mp 77−78 °C (ethanol); ^{1}H NMR δ 1.76 (m, 2H), 2.16 (m, 2H), 3.32 (t, 1H), 3.50−3.72 (m, 4H), 3.79−3.92 (m, 6H), 4.32 (dd, 1H), 4.53 (d, *J* = 7.82 Hz, 1H), 5.01 (m, 2H), 5.52 (s, 1H), 5.81 (m, 1H), 7.32−7.50 (m, 5H); ^{13}C NMR δ 138.12, 136.87, 129.24, 128.33, 126.43, 115.03, 101.99, 100.95, 78.42,78.28, 69.61, 68.72, 67.16, 67.00, 66.70, 29.97, 28.70.

Anal. Calcd for $C_{20}H_{26}O_6$: C, 66.28; H, 7.23. Found: C, 66.00; H, 7.28.

Pent-4-enyl 6-*O*-Benzyl-2,3-*O*-ethylene-*β*-D-glucopyranoside (6a). Pent-4-enyl 4,6-*O*-benzylidene-2,3-*O*-ethylene-*β*-D-glucopyranoside (**5*β***) (126.7 mg, 0.346 mmol) and $NaCNBH_3$ (195.7 mg, 3.11 mmol; 9 equiv) were stirred with anhydrous THF (7 mL) over freshly activated, powdered 3Å molecular sieves under argon. A saturated Et_2O/HCl solution (60 mL) was added until the solution stopped bubbling. Saturated aqueous $NaHCO_3$ (10 mL) was added, and the mixture was taken up in CH_2Cl_2 (125 mL) and subsequently washed with brine (2 × 50 mL). The water layer was re-extracted with CH_2Cl_2 (2 × 25 mL) and $CHCl_3$ (1 × 30 mL). The organic layers were combined, dried over Na_2SO_4, filtered, and evaporated to dryness. The residue was flash chromatographed (50% petroleum ether/EtOAc → 40% petroleum ether/EtOAc) to give **6a** (97.3 mg, 77%) as a colorless oil: $[\alpha]^{21}_D$ −55.5° (*c* 1.11, $CHCl_3$); ^{1}H NMR δ 1.79 (m, 2H), 2.13 (m, 2H), 2.92 (s, 1H), 3.32 (t, 1H), 3.50−3.72 (m, 4H), 3.79−3.92 (m, 6H), 4.41 (d, *J* = 7.57 Hz, 1H), 4.62 (d, 2H), 5.01 (m, 2H), 5.81 (m, 1H), 7.32−7.50 (m, 5H); ^{13}C NMR δ 138.03, 137.75, 128.50, 127.86, 127.75, 114.91, 100.49, 80.79, 78.42,76.86, 74.74, 73.69, 70.19, 69.58, 69.28, 66.96, 66.77, 30.04, 28.73.

Anal. Calcd for $C_{20}H_{28}O_6$: C, 65.92; H, 7.74. Found: C, 65.95; H, 7.55.

Pent-4-enyl 4,6-Di-*O*-benzyl-2,3-*O*-ethylene-*β*-D-glucopyranoside (6b). To a solution of pent-4-enyl 6-*O*-benzyl-2,3-*O*-ethylene-*β*-D-glucopyranoside (**6a**) (90.0 mg, 0.245 mmol) in DMF (4 mL) at 0 °C was added NaH (19.5 mg of a 60% dispersion in mineral oil, 0.49 mmol). After 10 min, benzyl bromide (0.010 mL, 0.49 mmol, 2 equiv) was added to the mixture, and the solution was allowed to slowly come to room temperature overnight. The reaction was quenched with methanol, taken up in EtOAc, washed with saturated aqueous $NaHCO_3$ (1 × 10 mL) and brine (2 × 15 mL), dried (Na_2SO_4), filtered, and evaporated to dryness. The residue was flash chromatographed to give **6b** (75.0 mg, 67%) as a clear, light yellow oil: $[\alpha]^{21}_D$ −7.73° (*c* 2.20, $CHCl_3$); ^{1}H NMR δ 1.79 (m, 2H), 2.12 (m, 2H), 3.32 (m, 1H), 3.50−3.72 (m, 4 H), 3.79−3.92 (m, 7H), 4.41 (d, *J* = 7.76 Hz, 1H), 4.51−4.62 (m, 3H), 4.87 (d, 1H), 5.01 (m, 2H), 5.81 (m, 1H), 7.22−7.50 (m, 10H); ^{13}C NMR δ 138.21, 138.11, 128.37, 127.96, 127.77, 127.73, 127.63, 114.88, 100.37, 82.19, 77.27, 75.42, 75.05, 74.57, 73.47, 72.13, 69.23, 68.98, 66.94, 66.80, 30.08, 28.77.

Anal. Calcd for $C_{27}H_{34}O_6$: C, 71.34; H, 7.45. Found: C, 71.40; H, 7.45.

Pent-4-enyl 2,6-Di-*O*-benzyl-*β*-D-glucopyranoside (7). According to the method of Garegg et al.,[21] pent-4-enyl 4,6-*O*-benzylidene-*β*-D-glucopyranoside **(3*β*)** (1.00 g, 2.97 mmol) was combined with *n*-butyltetraammonium hydrogen sulfate (0.200 g, 0.59 mmol, 0.2 equiv) and benzyl bromide (0.57 mL, 4.74 mmol, 1.6 equiv) in dichloromethane (55 mL). A 5% aqueous solution of NaOH (5 mL) was added, and the mixture was refluxed for 48 h. The solution was diluted with CH_2Cl_2 (25 mL), washed with brine (2 × 20 mL), dried (Na_2SO_4), filtered, and evaporated. The residue was flash chromatographed (85:15 light petroleum ether/EtOAc) to give a light yellow oil which consisted of an inseparable 3:1 mixture of the 2-*O*-benzyl and 3-*O*-benzyl regioisomers (1.0176, 80%). The mixture was directly treated with $NaCNBH_3$ (1.3438 g, 21.38 mmol, 9 equiv) in anhydrous THF (35 mL) under argon with 4 Å molecular sieves. A saturated HCl/Et_2O solution (250 mL) was added until the evolution of gas ceased. The reaction was quenched by slowly adding saturated aqueous $NaHCO_3$ (20 mL), and the mixture was diluted with CH_2Cl_2 (400 mL) and filtered through Celite. The layers were separated, and the aqueous layer was re-extracted with $CHCl_3$ (3 × 30 mL). The organic layers were combined, dried (Na_2SO_4), filtered, and evaporated. The residue was flash chromatographed (75:25 petroleum ether/EtOAc → 40:60 petroleum ether/EtOAc) to give **7** (605.1 mg, 59%) as a clear oil: $[\alpha]^{21}_D$ −5.98° (*c* 1.00, $CHCl_3$); ^{1}H NMR δ 1.79 (m, 2H), 2.18 (m, 2H), 2.99 (s, 1H), 3.19 (s, 1H), 3.22 (t, 1H), 3.50 (m, 4H), 3.70 (m, 2H), 3.93 (m, 1H) 4.40 (d, *J* = 7.76 Hz, 1H), 4.65 (m, 3H), 4.87 (d, 1H), 5.01 (m, 3H), 5.81 (m, 1H), 7.22−7.50 (m, 10H); ^{13}C NMR δ 138.31, 138.00, 137.92, 128.55, 128.47, 128.16, 127.94, 127.79, 127.74, 115.03, 103.31, 80.79, 76.06, 74.43, 74.15, 73.64, 71.40, 70.16, 69.37, 30.26, 28.98.

Anal. Calcd for $C_{25}H_{32}O_6$: C, 70.07; H, 7.53. Found: C, 70.00; H, 7.56.

Pent-4-enyl 2,6-Di-*O*-benzyl-3,4-*O*-ethylene-*β*-D-glucopyranoside (8). Pent-4-enyl 2,6-di-*O*-benzyl-*β*-D-glucopyranoside **(7)** (366.7 g, 0.858 mmol) was dissolved in dichloroethane (6 mL). Tetrabutylammonium hydrogen sulfate (58.2 mg, 0.171 mmol, 0.2 equiv) and a 35% aqueous NaOH solution (7 mL) were added, and the biphasic solution was stirred rapidly at 55 °C for 24 h. At this time, additional dichloroethane (3 mL) and NaOH solution (4 mL) were added, and the solution was stirred for another 24 h. The mixture was diluted with ethyl acetate (150 mL), washed with saturated aqueous $NaHCO_3$ (2 × 50 mL) and brine (1 × 75 mL), dried (Na_2SO_4), filtered, and evaporated. The residue was flash chromatographed (85:15 petroleum ether/EtOAc → 75:25 petroleum ether/EtOAc) to give **8** (246.7 mg, 63%) as a colorless oil: $[\alpha]^{21}_D$ −1.8° (*c* 1.25, $CHCl_3$); ^{1}H NMR *δ* 1.75 (m, 2H), 2.19 (m, 2H), 3.22−3.45 (m, 3H), 3.52−3.65 (m, 3H), 3.71−3.89 (m, 5H), 3.96 (m, 1H), 4.45 (d, *J* = 7.05 Hz, 1H), 4.61 (s, 2H), 4.78 (dd, 2H), 5.01 (m, 2H), 5.81 (m, 1H), 7.22−7.50 (m, 10H); ^{13}C NMR *δ* 138.54, 138.09, 128.35, 128.28, 127.88, 127.63, 127.57, 114.94, 103.59, 80.57, 78.84, 74.70, 74.41, 73.76, 73.53, 69.47, 68.82, 67.07, 66.79, 30.23, 28.97.

Anal. Calcd for $C_{27}H_{34}O_6$: C, 71.34; H, 7.54. Found: C, 71.23; H, 7.55.

Pent-4-enyl 2,3-*O*-(Octahydro-2,2′-bi-2*H*-pyran-2,2′-diyl)-*β*-D-glucopyranoside (9) and Pentenyl 3,4-*O*-(octahydro-2,2′-bi-2*H*-pyran-2,2′-diyl)-*β*-D-glucopyranoside (10). According to the method of Ley et al.,[22] a catalytic amount of camphorsulfonic acid (CSA; ca. 75 mg) was added to a stirred solution of pent-4-enyl *β*-D-glucopyranoside (**1*β*b**) (3.8010 g, 15.30 mmol) and bidihydropyran (4.8121 g, 28.96 mmol, 2.1 equiv) in dry, distilled $CHCl_3$. The mixture was refluxed for 7 h, and then the reaction was quenched by addition of ethyleneglycol (1.5 mL). The mixture was refluxed for an additional 0.5 h, and then it was diluted with CH_2Cl_2 (250 mL) and extracted with saturated aqueous $NaHCO_3$ (1 × 100 mL). The aqueous layer was re-extracted with CH_2Cl_2 (2 × 75 mL) and $CHCl_3$ (1 × 75 mL). The organic layers were combined, dried (Na_2SO_4), filtered, and concentrated. The residue was flash chromatographed (70:30 petroleum ether/EtOAc → 30:70 petroleum ether/EtOAc) to give **9** (1.9830 g, 4.78 mmol, 34%) and **10** (869.3 mg, 2.10 mmol, 15%) as light yellow foams. For **9**: $[\alpha]^{21}_D$ −83.3° (*c* 1.04, $CHCl_3$); R_f 0.2 (1:1 petroleum ether/EtOAc); ^{1}H NMR *δ* 1.32−1.87 (m, 16H), 2.08 (m, 2H), 3.41−3.82 (m, 11H), 3.92 (dd, 1H), 4.32 (d, *J* = 7.47 Hz, 1H), 4.97 (m, 2H), 5.83 (m, 1H); ^{13}C NMR *δ* 138.13, 114.87, 101.05, 96.80, 96.75, 76.07, 71.80, 69.46, 68.61, 67.79, 62.24, 60.72, 30.02, 28.88, 28.42, 28.36, 24.85, 24.78, 18.02.

Anal. Calcd for $C_{21}H_{34}O_8$: C, 60.85; H, 8.27. Found: C, 60.72; H, 8.26.

For **10:** $[\alpha]^{21}_D$ +37.3° (*c* 1.15, $CHCl_3$); R_f 0.5 (1:1 light petroleum ether/EtOAc); ^{1}H NMR *δ* 1.32−2.03 (m, 16H), 2.19 (m, 2H), 3.41−3.82 (m, 11H), 3.86 (dd, 1H) 4.54 (d, *J* = 7.90 Hz, 1H), 5.01 (m, 2H), 5.81 (m, 1H); ^{13}C NMR *δ* 138.02, 115.00, 103.56, 96.91, 96.80, 74.11, 71.35, 70.96, 69.74, 65.05, 61.50, 60.86, 60.74, 30.09, 28.68, 28.43, 28.38, 24.79, 24.74,18.02, 17.90.

Anal. Calcd for $C_{21}H_{34}O_8$: C, 60.85; H, 8.27. Found: C, 60.85; H, 8.34.

Pent-4-enyl 4,6-Di-*O*-benzyl-2,3-*O*-(octahydro-2,2′-bi-2*H*-pyran-2,2′-diyl)-*β*-D-glucopyranoside (11). Pent-4-enyl 2,3-*O*-(octahydro-2,2′-bi-2*H* pyran-2,2′-diyl)-*β*-D-glucopyranoside (**9**) (428.3 mg, 1.03 mmol) was dissolved in dry DMF at 0 °C under argon, and NaH (120 mg of a 60% dispersion in mineral oil, 2.99 mmol) was added. After 15 min, benzyl bromide (0.350 mL, 2.88 mmol) was added dropwise to the mixture, and the reaction was allowed to come slowly to room temperature overnight. The reaction was quenched with methanol, taken up in diethyl ether (60 mL), and washed consecutively with water (2 × 20 mL), saturated aqueous $NaHCO_3$ (1 × 25 mL), and brine (1 × 25 mL). The organic layer was dried (Na_2SO_4), filtered, and concentrated. The residue was flash chromatographed to give **11** (475.3 mg, 78%) as a white solid: mp 108−109 °C (ethanol); $[\alpha]^{21}_D$ −34.1° (*c* 1.31, $CHCl_3$); ^{1}H NMR *δ* 1.32−1.87 (m, 14H), 2.19 (m, 2H), 3.53 (m, 2H), 3.61 −3.82 (m, 8H), 3.95 (m, 2H) 4.49−4.64 (m, 4H), 4.95 (m, 3H), 5.83 (m, 1H), 7.18−7.39 (m, 10H); ^{13}C NMR *δ* 138.33, 138.27, 128.412, 128.34, 128.05, 127.77, 127.54, 114.76, 100.79, 96.88, 96.78, 75.53, 74.83, 73.46, 73.27, 69.27, 69.18, 68.81, 60.74, 30.15, 28.95, 28.55, 28.45, 24.94, 24.85, 18.42, 18.02.

Anal. Calcd for $C_{35}H_{46}O_8$: C, 70.68; H, 7.80. Found: C, 70.45; H, 7.82.

Pent-4-enyl 2,6-Di-*O*-benzyl-3,4-*O*-(octahydro-2,2′-bi-2*H*-pyran-2,2′-diyl)-*β*-D-glucopyranoside (12). Pent-4-enyl 3,4-*O*-(octahydro-2,2′-bi-2*H*-pyran-2,2′-diyl)-*β*-D-glucopyranoside (**10)** (235.0 mg, 0.567 mmol) was dissolved in dry DMF (6 mL) under argon at 0 °C, and NaH (68.0 mg of a 60% dispersion in mineral oil, 1.70 mmol) was added. After 15 min, benzyl bromide (0.202 mL) was added dropwise, and the solution was allowed to slowly come to room temperature overnight. The reaction was quenched with methanol and concentrated under high vacuum. The crude yellow solid was flash chromatographed (97.5:2.5 petroleum ether/EtOAc → 60:40 petroleum ether/EtOAc) to give **12** (288 mg, 85%) as a white solid: mp 104−105 °C (ethanol); $[\alpha]^{21}_D$ +23.1° (*c* 1.29, $CHCl_3$); ^{1}H NMR *δ* 1.47−2.00 (m, 14H), 2.19 (m, 2H), 3.45−3.70 (m, 6H), 3.71−3.91 (m, 4H), 3.96 (m, 2H), 4.42 (d, *J* = 7.45 Hz, 1H), 4.62 (m, 2H), 4.82 (m, 2H), 4.99 (m, 2H), 5.85 (m, 1H), 7.21−7.51 (m, 10H); ^{13}C NMR *δ* 138.18, 138.09, 128.39, 128.17, 127.70, 127.62, 127.45, 114.82, 103.72, 96.89, 96.73, 78.93, 74.66, 73.85, 73.55, 71.84, 69.44, 68.61, 65.40, 60.79, 60.62, 30.17, 28.90, 28.44, 24.79, 18.15, 17.94, 17.85.

Anal. Calcd for $C_{21}H_{34}O_8$: C, 70.68; H, 7.80. Found: C, 70.58; H, 7.76.

Pent-4-enyl 4,6-*O*-Benzylidene-2,3-*O*-(octahydro-2,2′-bi-2*H*-pyran-2,2′-diyl)-*β*-D-glucopyranoside (13). According to the method of Madsen and Fraser-Reid,[23] a solution of pent-4-enyl 2,3-*O*-(octahydro-2,2′-bi-2*H*-pyran-2,2′-diyl)-*β*-D-glucopyranoside **(9)** (515.7 mg, 1.243 mmol, previously coevaporated with toluene) and dipent-4-enyl benzaldehyde acetal (0.414 mL, 1.49 mmol) in acetonitrile (5 mL) was stirred with NBS (441 mg, 2.48 mmol, 2 equiv) and camphorsulfonic acid (28 mg) for 10 min at room temperature under argon. The reaction was quenched with Et_3N (20 mL), diluted with CH_2Cl_2 (20 mL), and washed with 10% aqueous sodium thiosulfate (1 × 10 mL) and saturated aqueous $NaHCO_3$ (1 × 10 mL). The organic layer was dried (Na_2SO_4), filtered, and evaporated. The residue was flash chromatographed (96:4 petroleum ether/EtOAc → 80:20 petroleum ether/EtOAc) to give **13** (449.8 mg, 72%) as a white foam: $[\alpha]^{21}_D$ −68.7° (*c* 1.00, $CHCl_3$); ^{1}H NMR *δ* 1.39−1.99 (m, 14H), 2.15 (m, 2H), 3.45−4.05 (m, 11H), 4.27 (dd, 1H), (d, *J* = 8.05 Hz, 1H), 4.95 (m, 2H), 5.51 (s, 1H), 5.80 (m, 1H), 7.21−7.51 (m, 5H); ^{13}C NMR *δ* 138.08, 137.45, 128.85, 128.40, 128.18, 126.32, 126.09, 114.9, 101.52, 100.99, 97.08, 96.74, 77.94, 69.68, 69.46, 68.74, 67.42, 61.13, 60.90, 60.64, 30.02, 28.91, 28.45, 25.17, 24.89, 18.05.

Anal. Calcd for $C_{28}H_{38}O_8$: C, 66.91; H, 7.62. Found: C, 66.65; H, 7.67.

Acknowledgment. We are grateful to the National Science Foundation (CHE 9311356) and Glaxo Research Institute for financial support of this work. We thank Professor A. T. McPhail for the X-ray structure shown in Figure 1.

JO9601223